



HAL
open science

Recommended Nuclear Data for the Production of Selected Therapeutic Radionuclides

J.W. Engle, A.V. Ignatyuk, R. Capote, B.V. Carlson, A. Hermanne, A.
Kellett, T. Kibédi, G. Kim, G. Kondev, M. Hussain, et al.

► **To cite this version:**

J.W. Engle, A.V. Ignatyuk, R. Capote, B.V. Carlson, A. Hermanne, et al.. Recommended Nuclear Data for the Production of Selected Therapeutic Radionuclides. Nuclear Data Sheets, 2019, 155, pp.56-74. 10.1016/j.nds.2019.01.003 . cea-02163921

HAL Id: cea-02163921

<https://cea.hal.science/cea-02163921>

Submitted on 24 Jun 2019

HAL is a multi-disciplinary open access archive for the deposit and dissemination of scientific research documents, whether they are published or not. The documents may come from teaching and research institutions in France or abroad, or from public or private research centers.

L'archive ouverte pluridisciplinaire **HAL**, est destinée au dépôt et à la diffusion de documents scientifiques de niveau recherche, publiés ou non, émanant des établissements d'enseignement et de recherche français ou étrangers, des laboratoires publics ou privés.

Recommended Nuclear Data for the Production of Therapeutic Radionuclides

J. W. Engle,^{1,*} A. V. Ignatyuk,² R. Capote,^{3,†} B. V. Carlson,⁴ A. Hermanne,⁵ M. A. Kellett,⁶
 T. Kibédi,⁷ G. Kim,⁸ F. G. Kondev,⁹ M. Hussain,¹⁰ O. Lebeda,¹¹ A. Luca,¹² Y. Nagai,¹³ H. Naik,¹⁴
 A. L. Nichols,¹⁵ F. M. Nortier,¹ S. V. Suryanarayana,¹⁴ S. Takács,¹⁶ F. T. Tárkányi,¹⁶ and M. Verpelli³

¹Los Alamos National Laboratory (LANL), USA

²Institute of Physics and Power Engineering (IPPE), Obninsk, Russia

³NAPC–Nuclear Data Section, International Atomic Energy Agency, Vienna, Austria

⁴Instituto Tecnológico de Aeronáutica, Brazil

⁵Cyclotron Department - TONA, Vrije Universiteit Brussel, Brussels, Belgium

⁶CEA, LIST, Laboratoire National Henri Becquerel (LNE-LNHB), France

⁷Australian National University (ANU), Canberra, Australia

⁸Kyungpook National University, Republic of Korea

⁹Argonne National Laboratory (ANL), USA

¹⁰Government College University, Lahore, Pakistan

¹¹Nuclear Physics Institute, Rez, Czech Republic

¹²National Institute of Physics and Nuclear Engineering “Horia Hulubei”, Romania

¹³Japan Atomic Energy Agency (JAEA), Tokaimura Naka, Ibaraki-ken, Japan

¹⁴Bhabha Atomic Research Centre (BARC), Trombay, Mumbai, India

¹⁵University of Surrey, Guildford, UK

¹⁶Institute for Nuclear Research, Debrecen, Hungary

(Received 10 August 2018; revised received xxx October 2018; accepted XX 2018)

Increasing interest in the treatment of human disease using targeted radionuclide-based therapies requires accurate understanding of achievable radionuclide yield and purity. In the frame of a larger International Atomic Energy Agency Coordinated Research Proposal (IAEA CRP), thirteen nuclear reactions leading to the formation of ^{131}Cs , ^{178}Ta , ^{225}Ra , ^{225}Ac , ^{227}Th , and ^{230}U have been evaluated using all available measured data. Selected datasets have been fit using least-squares method with Padé approximations of variable order, enabling the assignment of energy differential uncertainties to the recommended fit. In some instances, new measurements have been made and reported data has been adjusted to accommodate new nuclear decay or monitor reaction data which adversely altered original reported quantities. In many additional cases, insufficient measured data are available to permit a reliable evaluation of cross sections; these instances are discussed. Recommended therapeutic radionuclide production reaction data and their uncertainties are available on the Web page of the IAEA NDS at www-nds.iaea.org/radionuclides/ and also at the IAEA medical portal www-nds.iaea.org/medportal/.

CONTENTS

	A. $^{131}\text{Xe}(p,n)^{131}\text{Cs}$	3
	B. $^{133}\text{Cs}(p,3n)^{131}\text{Ba}$ (100% EC decay) ^{131}Cs	4
I. INTRODUCTION		2
A. IAEA Objectives		2
B. Dataset Selection and Fitting Considerations		3
C. Therapeutic Radionuclide Productions Investigated		3
II. Production of ^{131}Cs		3
	III. Production of ^{178}Ta	5
	A. $^{nat}\text{Ta}(d,xn)^{178}\text{W}$	5
	B. $^{nat}\text{Ta}(p,xn)^{178}\text{W}$	6
	C. $^{nat}\text{Hf}(\alpha,xn)^{178}\text{W}$	6
	IV. Production of ^{225}Ac	7
	A. $^{232}\text{Th}(p,x)^{225}\text{Ac}$	7
	B. $^{226}\text{Ra}(p,2n)^{225}\text{Ac}$	8
	C. $^{232}\text{Th}(p,x)^{225}\text{Ra}$ (100% β^- decay) ^{225}Ac	9
	V. Production of ^{227}Th	10
	A. $^{232}\text{Th}(p,x)^{227}\text{Th}$	10
	B. $^{232}\text{Th}(p,x)^{227}\text{Ac}$ (98.62% β^- decay) ^{227}Th	11

* New institutional affiliation: University of Wisconsin, Madison, Wisconsin, USA; jwengle@wisc.edu

† Corresponding author email: r.capoteny@iaea.org

VI. Production of ^{230}U	12
A. $^{231}\text{Pa}(p,2n)^{230}\text{U}$	12
B. $^{231}\text{Pa}(d,3n)^{230}\text{U}$	12
C. $^{232}\text{Th}(p,3n)^{230}\text{Pa}$ (7.80% β^- decay) ^{230}U	13
VII. SUMMARY AND CONCLUSIONS	14
Acknowledgements	14
References	14

I. INTRODUCTION

A. IAEA Objectives

Several decades of concentrated research and development for medically diagnostic radionuclides have increasingly created opportunities for radionuclides in therapeutic applications. The production of these radionuclides is an important non-energy related application of nuclear science and technology. Reliable and high-quality nuclear data are essential to guarantee safe and efficient therapeutic treatments [1–3]. Therapeutic radionuclides are commonly produced via reactions induced by charged and neutral particles. Especially as the number of therapeutic radionuclides under study has expanded, the variety of relevant reactions has also grown, and in many cases measured data sets reported in the literature are discrepant from one other. An effort was made to formally reconcile these differences through expert evaluation of the data in a Coordinated Research Project (CRP) of the International Atomic Energy Agency (IAEA) that concluded in 2010, which made available dedicated compilations and evaluations of data for all charged-particle induced reactions contributing to the production of ^{64}Cu , ^{67}Cu , ^{67}Ga , ^{86}Y , ^{103}Pd , ^{111}In , ^{114m}In , ^{124}I , ^{125}I , ^{169}Yb , ^{177}Lu , ^{186}Re , ^{192}Ir , ^{211}At , and ^{225}Ac (35 reactions were considered) [4]. These data were made available via institutional publication and in an online repository that is used extensively by the radionuclide production community. But some of those evaluations are no longer current, as new measurements are made constantly and additional reactions and products have received attention [5, 6].

For this reason, a new CRP was initiated to provide dedicated evaluations of data for charged particle induced reactions divided into three primary thrusts: monitor reactions, reactions to produce diagnostic radionuclides, and reactions to produce therapeutic radionuclides. Three meetings were held [7–9]; sixteen institutions worldwide contributed to this effort. The continuing mission of the IAEA and its relevance to accelerator production of radionuclides in general receives thorough discussion in the first publication resulting from the CRP [10]. In addition to the evaluation of cross section data, significant effort was also invested in evaluations and new measurements of nuclear decay data that will be published elsewhere. Evaluations were supported when possible with new cross-section measurements. All available sources of data were considered, and each source was examined rigorously to confirm that beam intensities and energies, target materials, and experimental uncertainties were accurately and completely described. The thirteen reactions summarized here lead to the production of ^{131}Cs , ^{178}Ta , ^{225}Ra , ^{225}Ac , ^{227}Th , and ^{230}U .

B. Dataset Selection and Fitting Considerations

Selected experimental excitation functions were fitted using a least-squares method with Padé approximants [11–13]. This method of fitting enables estimation of the uncertainty in the reported fits [14, 15], which is given in all cases below. Note that current evaluations are overwhelmingly based on fit to the selected experimental data alone (very few exceptions discussed below). For detailed discussion of the methodology used to perform the fitting, the reader is referred to the thorough treatment in the first publication resulting from the current CRP [10]. Predicted instantaneous and saturation yields were calculated using the evaluated data (Padé fit) and are also reported. Here “instantaneous” refers to yield from an irradiation of infinitesimal duration, while “saturation” refers to yield from an irradiation of infinite duration, when the rates of production and radioactive decay are essentially equivalent. Where possible and useful, yields for monoisotopic targets have been extrapolated from experiments that used targets of natural isotopic abundance.

C. Therapeutic Radionuclide Productions Investigated

The reactions summarized in Table 1 have been examined, and nuclear data is recommended for each in the sections that follow. In several cases, it is possible to form the radionuclide of interest by direct reactions and also by the production of its radioactive parent, which can then be used as feedstock material. For example, ^{178}Ta is formed from the decay of ^{178}W , which can be produced by proton irradiation of tantalum targets via a reaction that has been measured. Throughout, nuclear data used comes from the National Nuclear Data Center’s repository [16] (as evaluated within the ENSDF network [17]) unless otherwise noted.

II. PRODUCTION OF ^{131}Cs

The X-ray and Auger-electron emitter ^{131}Cs ($T_{1/2} = 9.689$ d, 100% EC) has been of interest as a radioactive source for brachytherapy and stereotactic surgery implants since the mid 1960s, with interest increasing especially following the commercialization of reactor-based production methods [18]. Its primary X-ray energy (29 keV) and half-life are comparable to that of ^{103}Pd , whose commercial production using cyclotrons is well established, and the slightly higher energy photon emitted by ^{131}Cs is thought to deliver more uniform dose than ^{103}Pd in certain clinical situations [19]. Accelerator production is possible via several routes, two of which were evaluated: direct production by $^{131}\text{Xe}(p,n)^{131}\text{Cs}$ and indirect production at higher energies with $^{133}\text{Cs}(p,3n)^{131}\text{Ba}$ (100% EC decay) ^{131}Cs .

TABLE I. Reactions and decay data of activation products under investigation ($T_{1/2}$ is product half-life, and E is emission energy (keV) with emission probability of I (%), as taken from NuDat [16]).

Reaction	$T_{1/2}$	Principal Emission	E (keV) (I(%)) ^a
$^{131}\text{Xe}(p,n)^{131}\text{Cs}$	9.689 d	Auger e ⁻	3.43 (79.7)
$^{133}\text{Cs}(p,3n)^{131}\text{Ba}$ $\Rightarrow(\text{EC})^{131}\text{Cs}$	11.50 d (^{131}Ba)	γ	123.804 (29.8) 216.88 (20.4) 496.321 (48.0)
$^{nat}\text{Ta}(d,xn)^{178}\text{W}$ $\Rightarrow(\text{EC})^{178}\text{Ta}$	21.6 d ^b (^{178}W)	Auger e ⁻	6.35 (54)
$^{nat}\text{Ta}(p,xn)^{178}\text{W}$ $\Rightarrow(\text{EC})^{178}\text{Ta}$	21.6 d ^b (^{178}W)	Auger e ⁻	6.35 (54)
$^{nat}\text{Hf}(\alpha,xn)^{178}\text{W}$ $\Rightarrow(\text{EC})^{178}\text{Ta}$	21.6 d ^b (^{178}W)	Auger e ⁻	6.35 (54)
$^{232}\text{Th}(p,x)^{225}\text{Ac}$	9.92 d ^c	α (90%)	5830 (50.7)
$^{226}\text{Ra}(p,2n)^{225}\text{Ac}$	9.92 d ^c	α (90%)	5830 (50.7)
$^{232}\text{Th}(p,x)^{225}\text{Ra}$ $\Rightarrow(\beta^-)^{225}\text{Ac}$	14.9 d (^{225}Ra)	β^- (100%)	316 (69.5) 356 (30.5)
$^{232}\text{Th}(p,x)^{227}\text{Th}$	18.697 d	α (100%)	6038.1 (24.2)
$^{232}\text{Th}(p,x)^{227}\text{Ac}$ $\Rightarrow(\beta^-)^{227}\text{Th}$	21.772 y (^{227}Ac)	β^- (98.620%)	20.3 (10.0) 35.5 (35) 44.8 (54)
$^{231}\text{Th}(p,2n)^{230}\text{U}$	20.8 d	α (100%)	5888.4 (67.4)
$^{231}\text{Th}(d,3n)^{230}\text{U}$	20.8 d	α (100%)	5888.4 (67.4)
$^{232}\text{Th}(p,3n)^{230}\text{Pa}$ $\Rightarrow(\beta^-)^{230}\text{U}$	17.4 d (^{230}Pa)	β^- (7.8%)	508 (7.6)

^a Decay data taken from Refs. [16, 17]; mean Auger-electron emission energies and β^- end-point energies listed.

^b ^{178}W (0^+) ground state undergoes 100% EC decay to low-spin (1^+) isomer of ^{178}Ta ($T_{1/2}$ of 9.38 min.)

^c ^{225}Ac half-life of 9.92 d adopted from the recent measurement of Pommé *et al.* [20].

A. $^{131}\text{Xe}(p,n)^{131}\text{Cs}$

Only a single dataset exists that describes $^{131}\text{Xe}(p,n)^{131}\text{Cs}$ [21], covering the energy range from threshold to 28 MeV. Additional experimental measurements are needed, but agreement of theoretical predictions with measured data is acceptable. No data were deselected or adjusted, and the selected data are well-represented by the Padé fit of 11 parameters to the available 27 data points, evaluated and shown in Figure 1. Fitting uncertainties are highest at low energies where the measured energy of the proton beam is itself most uncertain, but fall to 6% by 10 MeV before rising slowly to 10% above 25 MeV. Systematic uncertainty is added as 5% of fitted values. Instantaneous yields calculated from the fitted function are shown in Figure 2.

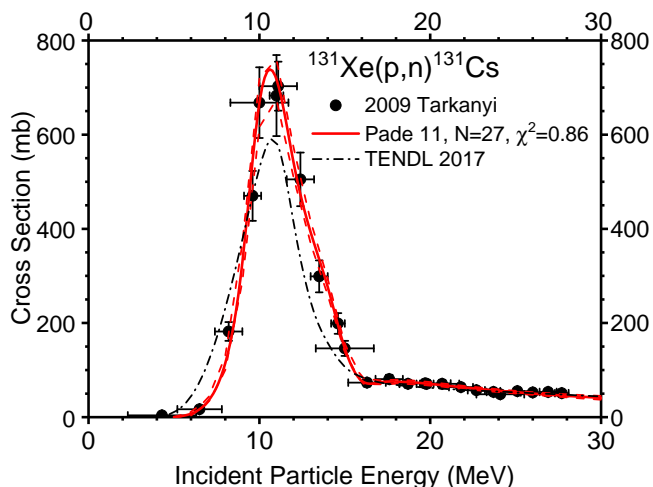


FIG. 1. (Color online) Evaluated Padé fit and TENDL-2017 evaluation are compared with experimental data from Ref. [21] for the $^{131}\text{Xe}(p,n)^{131}\text{Cs}$ reaction.

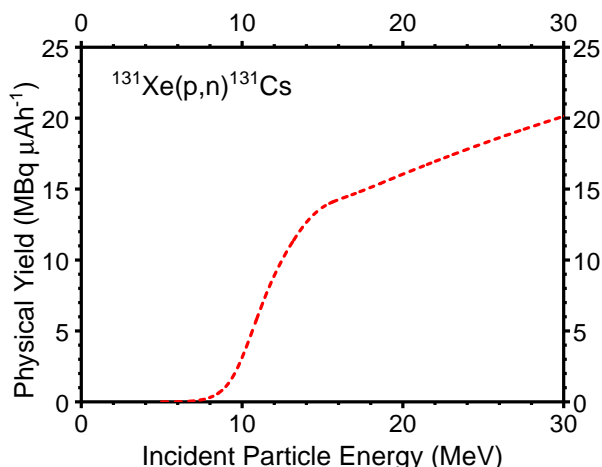
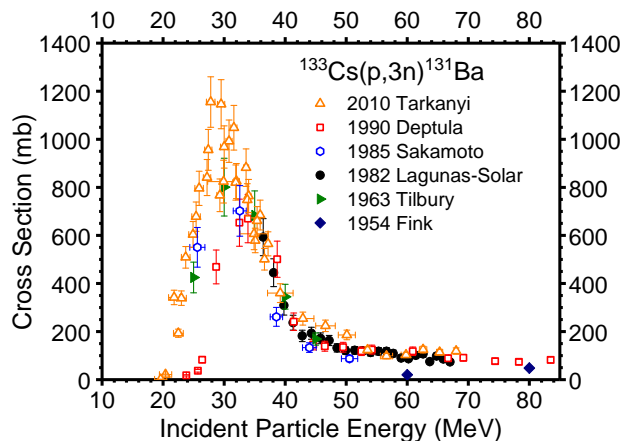


FIG. 2. (Color online) Physical yields calculated from Padé fit of data selected for the $^{131}\text{Xe}(p,n)^{131}\text{Cs}$ reaction.

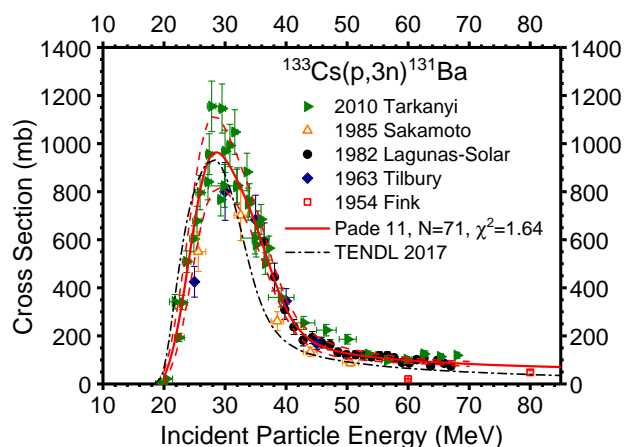
B. $^{133}\text{Cs}(p,3n)^{131}\text{Ba}$ (100% EC decay) ^{131}Cs

Production of ^{131}Cs is also possible using the ground state isomer of its radioactive parent, ^{131}Ba ($T_{1/2} = 11.50$ d, 100% EC) as a feedstock of carrier-free ^{131}Cs radiochemical isolation strategies. The same technique is employed in reactor environments, which access ^{131}Ba via the $^{130}\text{Ba}(n,\gamma)^{131}\text{Ba}$ neutron capture reaction. For the proton-induced reaction, available data plotted in Figure 3(a) describe a threshold energy near 20 MeV with a peak excitation function near 1000 mb and 30 MeV. The tail of the excitation function asymptotically approaches 70 mb above 70 MeV incident proton energy. Six datasets describe the reaction [22–27]. Only the dataset from Deptula et al. [23] was deselected due to its obvious energy shift at low incident proton energies. An 11-parameter Padé fit was chosen to represent the remaining 71 data points plotted in Figure 3(b), giving a χ^2 of 1.64. Instantaneous yields calculated from the fitted function are shown

in Figure 4, rising rapidly up until the peak of the excitation function is passed near 40 MeV and continuing to rise with energy as the high energy tail of the excitation function remains near 100 mb until 80 MeV.



(a) All experimental data are plotted with uncertainties.



(b) Selected data compared with evaluated Padé fit and TENDL-2017 data up to 85 MeV.

FIG. 3. (Color online) Evaluated Padé fit and TENDL-2017 data are compared with experimental data from Refs. [22, 24–27] for the $^{133}\text{Cs}(p,3n)^{131}\text{Ba}$ reaction.

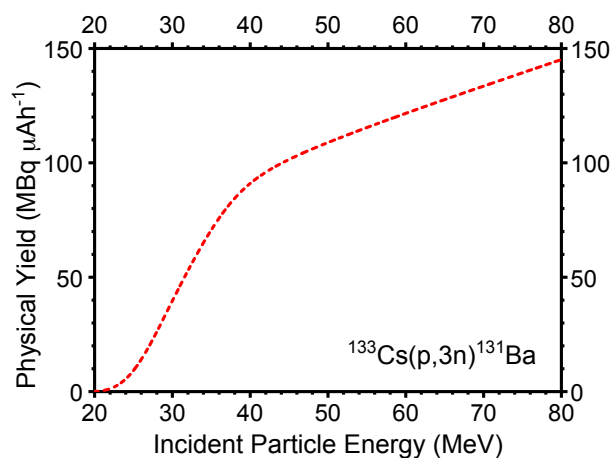


FIG. 4. (Color online) Physical yields calculated from Padé fit of evaluated data for the $^{133}\text{Cs}(p,3n)^{131}\text{Ba}$ reaction.

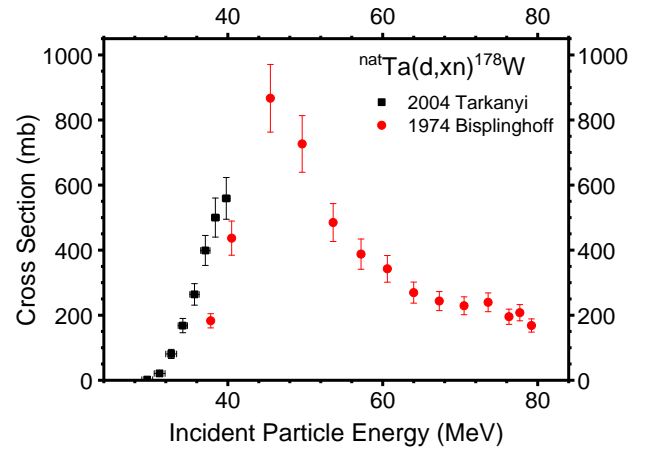
Though proton irradiation of isotopically enriched ^{131}Xe affords a production possibility with the globally-distributed fleet of low energy cyclotrons, the constraints imposed on accelerators and radiochemistry by enriched gas targets make the $^{133}\text{Cs}(p,3n)^{131}\text{Ba}$ relatively more attractive. Irradiations of ^{133}Cs have higher yields and can employ solid targets of natural isotopic abundance in exchange for only moderate added complexity in the radiochemical isolation process, since both ^{131}Ba and ^{131}Cs will have to be recovered in succession.

III. PRODUCTION OF ^{178}Ta

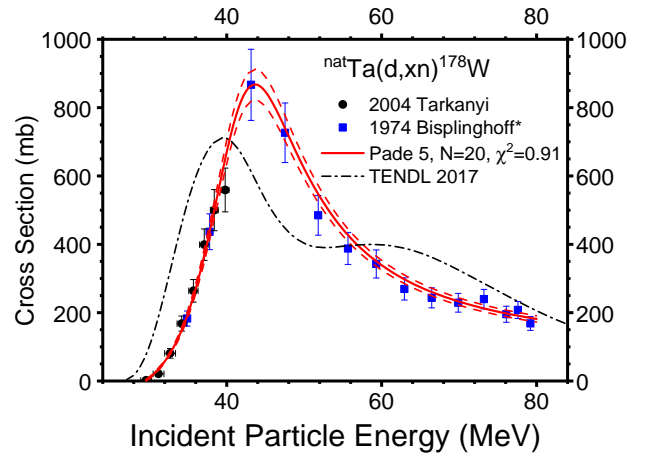
The short-lived ($T_{1/2} = 9.3$ min) metastable state of the ^{178}Ta radioisotope can be used both for diagnostic (positron emission tomography imaging, via a total β^+ decay intensity of 1.24%) as well as for therapeutic purposes [28]. The rapid decay of ^{178}Ta motivates indirect production routes that make use of its radioactive parent's longer half-life (^{178}W , $T_{1/2} = 21.6$ d, 100% EC) to afford multiple elutions of ^{178}Ta from radioisotope generators [29, 30]. These multiple elutions can make sequential imaging studies convenient, especially in applications where repeated assays are required, e.g., quantification of ventricular function in preclinical subjects [31].

A. $^{nat}\text{Ta}(d,xn)^{178}\text{W}$

Two complementary datasets were found for $^{nat}\text{Ta}(d,xn)^{178}\text{W}$ [32, 33] and are shown in Figure 5(a). The two experiments exhibit disagreement in energy near 40 MeV. Because the data from Bisplinghoff et al. [32] were measured after degrading the incident deuteron beam from an initial energy of 80 MeV, this dataset was systematically shifted lower in energy to match the data from Tarkanyi et al. [33] (Figure 5(b)). No other adjustments were made prior to fitting, which was accomplished with a 5 parameter Padé fit of 20 data points ($\chi^2=0.91$). The shape of the TENDL-2017 data above 50 MeV is remarkable, since no obvious physical explanation exists for the local maximum predicted near 60 MeV. This feature is contradicted by the more expected shape of the measured data. Relative uncertainty in the Padé fit is 10% except for the lowest two energy points used, and a systematic uncertainty of 4% has been added throughout. Physical yields using the recommended fit have been calculated and are shown in Figure 6. Because the yield is increasing with energy at a nearly constant rate throughout the energy range considered, and because no tungsten radioisotopes with long half lives exist to reduce the radioisotopic purity of ^{178}W , irradiations with higher incident energy deuterons are favored.



(a) All experimental data are plotted with uncertainties.



(b) Selected data compared with evaluated Padé fit and TENDL-2017 data up to 80 MeV.

*Data from Ref. [32] have been shifted in energy to account for systematic disagreement with data from Ref. [33].

FIG. 5. (Color online) Evaluated Padé fit and TENDL-2017 evaluation are compared with experimental data from Refs. [32, 33] for the $^{nat}\text{Ta}(d,xn)^{178}\text{W}$ reaction.

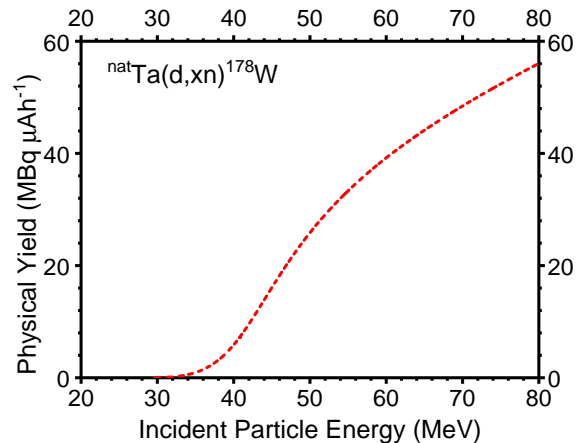
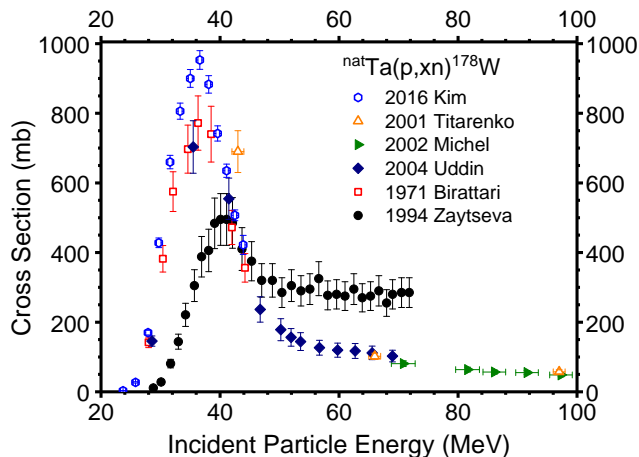
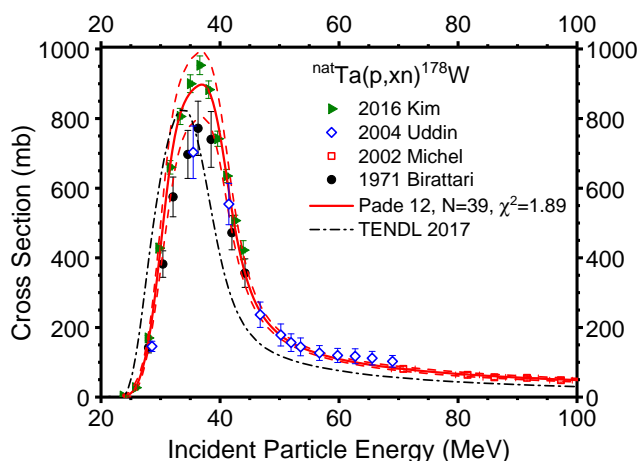


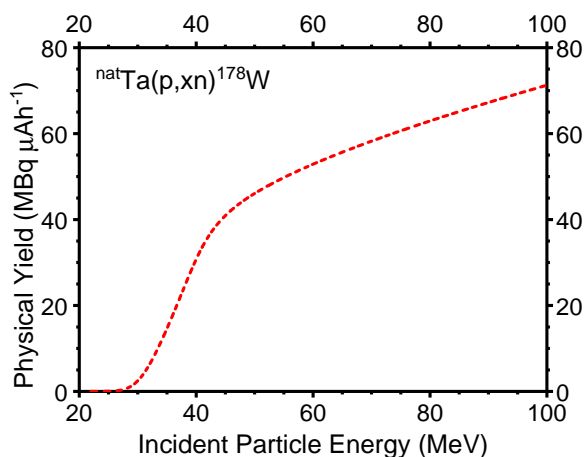
FIG. 6. (Color online) Physical yields calculated from Padé fit of data selected for the $^{nat}\text{Ta}(d,xn)^{178}\text{W}$ reaction.



(a) All experimental data are plotted with uncertainties.



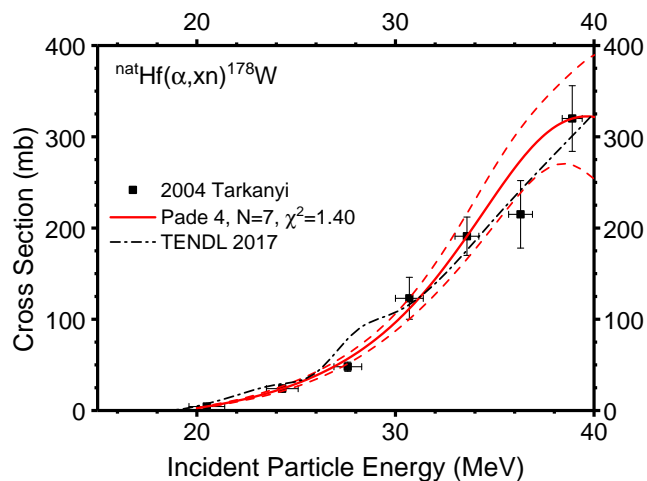
(b) Selected data compared with evaluated Padé fit up to 80 MeV.

FIG. 7. (Color online) Evaluated Padé fit and TENDL-2017 evaluation are compared with experimental data from Refs. [34–39] for the $^{nat}\text{Ta}(p,xn)^{178}\text{W}$ reaction.FIG. 8. (Color online) Physical yields calculated from Padé fit of data selected for the $^{nat}\text{Ta}(p,xn)^{178}\text{W}$ reaction.B. $^{nat}\text{Ta}(p,xn)^{178}\text{W}$

Proton induced reactions on targets of ^{nat}Ta are described by six reported measurements [34–39]. Measurements describe an excitation very similar in magnitude and energy to the deuteron induced route described above, shown in Figure 5(a). The excitation function's single maximum occurs between 35 and 40 MeV, and the width of the principle peak from the $^{181}\text{Ta}(p,4n)^{178}\text{W}$ reaction is approximately 15 MeV FWHM. The data from Zaytseva et al. [35] and Titarenko et al. [39] are deselected for their obvious energy shifts and as outliers from other data, and no other data are modified. Using the selected 39 data points, a 12 parameter Padé fit achieves a $\chi^2=1.89$. All evaluated data are compared with selected data and the Padé fit in Figure 7(b). The tail of the excitation function has a declining magnitude <100 mb above 80 MeV, and no discernible feature from $^{180}\text{Ta}(p,5n)^{178}\text{W}$ can be detected because of the small abundance of the target in tantalum of natural isotopic composition (0.012%). The uncertainty in the recommended fit includes a systematic contribution of 5%, and declines from approximately 10% at low energies to a minimum near 50 MeV of 6%, before rising again to 9% at 100 MeV. Physical yields using the recommended fit have been calculated and are shown in Figure 8.

C. $^{nat}\text{Hf}(\alpha,xn)^{178}\text{W}$

Available data describing alpha induced reactions that form ^{178}W are extremely limited. Only a single measurement was found by the CRP; the report from Tarkanyi et al. [33] of the $^{nat}\text{Hf}(\alpha,xn)^{178}\text{W}$ reaction contains 7 data points spanning the energy range between 20 and 40 MeV. This measured data, which appears to be rising towards the excitation function's maximum near 40 MeV, was fit with a 4 parameter Padé representation giving a $\chi^2=1.40$.

FIG. 9. Evaluated Padé fit and TENDL-2017 evaluation are compared with experimental data from Ref. [33] for the $^{nat}\text{Hf}(\alpha,xn)^{178}\text{W}$ reaction.

The contribution of reactions on hafnium isotopes with mass numbers 176, 177, and 178 are tentatively visible in the structure of the TENDL 2017 evaluation between 20 and 25 MeV, 25 and 30 MeV, and above 30 MeV (see Ref. 9), but large uncertainty and a lack of data mean that experimental measurements are unable to verify the theoretical prediction in this regard. The lack of experimental data with information on the behavior of the excitation function near its peak causes the uncertainty of the recommended fit to increase rapidly above the final data point at 40 MeV; no recommendation is made at higher energies. Physical yields calculated from the Padé fit are two orders of magnitude lower than those for proton or deuteron induced reactions on tantalum targets (Figure 10). Such a large yield reduction subjugates the considerations of ^{178}W 's radiochemical isolation, especially given that targets of isotopically enriched hafnium would be desirable to mitigate co-production of long-lived tantalum radioisotopes (e.g., ^{182}Ta , $T_{1/2} = 114.43$ d) as waste, making irradiations of tantalum targets a putatively superior choice.

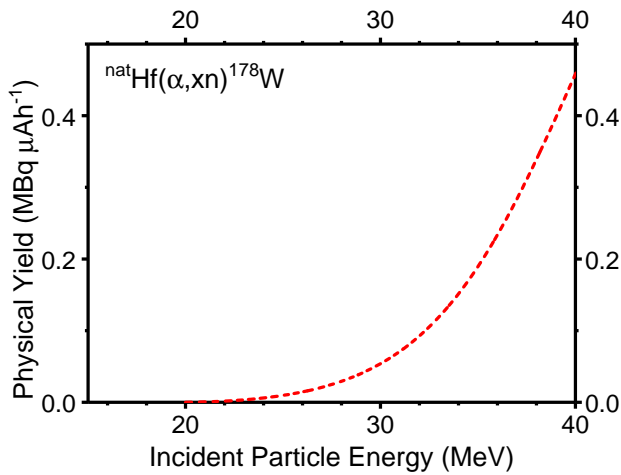


FIG. 10. (Color online) Physical yields calculated from Padé fit of data selected for the $^{nat}\text{Hf}(\alpha, xn)^{178}\text{W}$ reaction.

IV. PRODUCTION OF ^{225}Ac

The alpha-emitting radionuclide ^{225}Ac ($T_{1/2} = 9.92$ d, 100% α) has been identified as one of the most promising candidates for radiotherapeutic medical applications because 4 different alpha particles are emitted along its decay chain to stable ^{209}Bi , potentially depositing a very intense radiation dose in a relatively small volume of tissue. The current global supply of ^{225}Ac is almost entirely sourced from generators of ^{225}Ac 's radioactive grandparent ^{229}Th ($T_{1/2} = 7392$ y, 100% α) [40]. These generators are typically eluted every 4-8 weeks, recovering both ^{225}Ac and its parent, ^{225}Ra ($T_{1/2} = 14.9$ d, 100% β^-). The ^{225}Ra can be chemically processed subsequently to recover additional ^{225}Ac . The generators thus provide approximately 2 Ci of ^{225}Ac per year, which is insufficient to

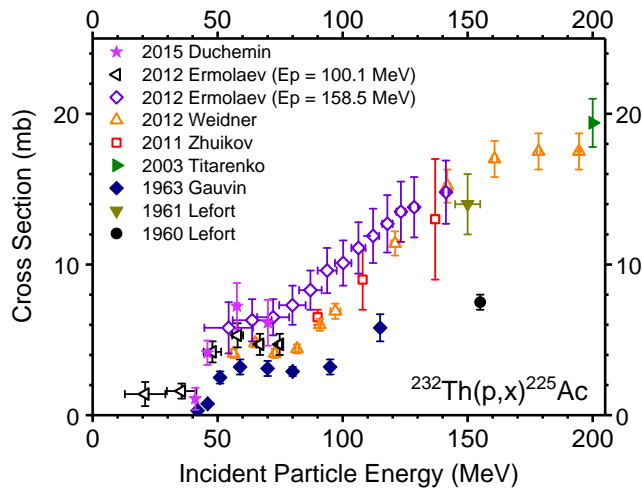
meet the anticipated demands of large scale clinical trials needed for ^{225}Ac -based radiopharmaceuticals to move reliably into clinical applications. Besides the charged-particle induced reactions considered below, additional, less-studied options exist to increase the global stockpile of ^{229}Th (e.g., $^{232}\text{Th}(p, x)^{229}\text{Th}$) or using neutral particle fluxes to form ^{225}Ac indirectly (e.g., $^{226}\text{Ra}(n, 2n)^{225}\text{Ra}$ and $^{226}\text{Ra}(\gamma, n)^{225}\text{Ra}$), but these reactions are beyond the scope undertaken for the present work.

The decay of ^{225}Ac also leads to ^{213}Bi ($T_{1/2} = 45.6$ min, 98% β^- , 2% α) and the emission of a single alpha particle either following β^- -decay to ^{213}Po or α -decay to ^{209}Tl . These alpha emissions have made ^{213}Bi a useful radiolabel for a variety of clinical studies and stimulated consideration of ^{225}Ac as generator feedstock in its own right. The cellular lethality of its single alpha emission is significantly lower than ^{225}Ac 's, which requires larger injected activities for therapeutic effects and higher yields from accelerator efforts to support even pre-clinical research endeavors.

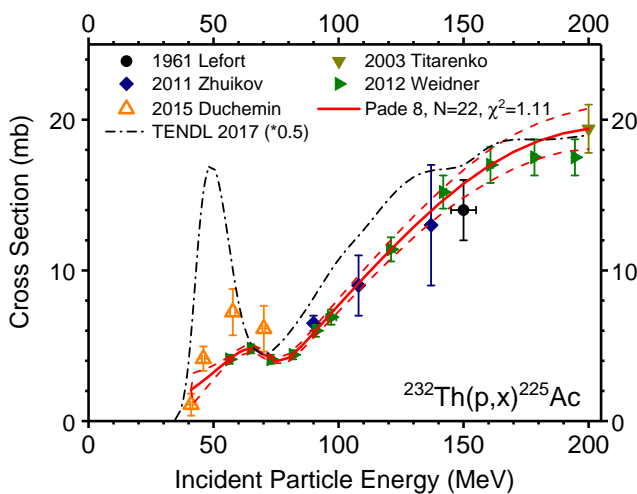
Three reaction routes to ^{225}Ac are considered below, all using proton-induced reactions: direct production via $^{232}\text{Th}(p, x)^{225}\text{Ac}$ and $^{226}\text{Ra}(p, 2n)^{225}\text{Ac}$, and indirect production via $^{232}\text{Th}(p, x)^{225}\text{Ra}$ (100% β^- decay) ^{225}Ac . Reactions on targets of ^{232}Th require higher incident energies and therefore consideration of more numerous possible side reactions.

A. $^{232}\text{Th}(p, x)^{225}\text{Ac}$

The only direct production route to ^{225}Ac that uses a stable target is the $^{232}\text{Th}(p, x)^{225}\text{Ac}$ reaction, which has an approximate threshold near 40 MeV. This route was first explored in the 1950s and 1960s with single point measurements by four groups [41–45] mostly at higher energies than those considered by this evaluation. A total of 12 datasets were found in 10 publications using incident proton energies up to 1.2 GeV, and an additional measurement of thick target yields has been completed since data were evaluated [46]. This evaluation includes only data up to 200 MeV; these are shown in Figure 11(a) [42, 43, 45, 47–51], omitting data at higher energies from Refs. [41, 43, 44, 48]. Data shown includes the measurements made by Ermolaev et al. [49] using targets of thorium so thick that the usual assumption of a monoenergetic proton beam was rendered invalid; for this reason these data (from two separate experiments) were deselected. Finally, the dataset of Gauvin [42] was deselected during fitting because of its significant contradiction other measured data and unresolved questions concerning proton beam intensity monitoring during the experiment. The evaluated and selected data (22 data points) are summarized with an 8 parameter Padé fit as shown in Figure 11(b). Some structure in the excitation function is observed between 40 and 80 MeV, likely corresponding to the emission of alpha particles as secondary ejectiles. The selected datasets disagree on the magnitude of this



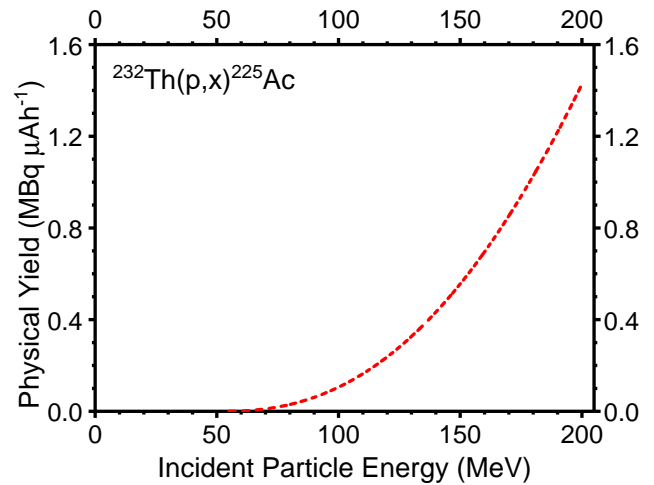
(a) All experimental data are plotted with uncertainties.



(b) Selected data compared with evaluated Padé fit and TENDL-2017 data up to 200 MeV.

FIG. 11. (Color online) Evaluated Padé fit and TENDL-2017 evaluation are compared with experimental data from Refs. [42, 43, 45, 47–51] for the $^{232}\text{Th}(p,x)^{225}\text{Ac}$ reaction. TENDL-2017 data are scaled in magnitude with the factor shown to enable comparison with measured data.

reaction channel near 60 MeV, and theoretical data from TENDL 2017, also plotted in 11(b), predicts a magnitude for the entire excitation function that more than doubles measured values. As a result, the combination of fitted and experimental systematic uncertainties exceeds 10% in the energy region below 80 MeV, but at higher energies the recommended uncertainty is in all cases below 8%. The small number of datasets and their general inhomogeneity suggests a strong need for additional experimental measurements. Fitted data were used to calculate the physical yield of the $^{232}\text{Th}(p,x)^{225}\text{Ac}$ reaction (Figure 12), which is increasing with energy over the range of energies studied, suggesting higher energy incident protons for the production of large activities of ^{225}Ac .

FIG. 12. (Color online) Physical yields calculated from Padé fit of data selected for the $^{232}\text{Th}(p,x)^{225}\text{Ac}$ reaction.

B. $^{226}\text{Ra}(p,2n)^{225}\text{Ac}$

With this constraint, an 8 parameter Padé fit achieves a $\chi^2=0.02$ for the 5 experimental data points + 4 added theoretical data points. Relative uncertainty in the fitted function is high, above 20% at energies below 13 MeV and between 10 and 20% across the remaining range of energies examined. Plotted yields (Figure 14) point to sub-25 MeV incident energy irradiations given the consideration of target material handling and recovery, with more moderate gains above the peak of the excitation function near 20 MeV. To date, only a single experimental measurement of the $^{226}\text{Ra}(p,2n)^{225}\text{Ac}$ reaction excitation function has been performed [52]. Use of this reaction is extremely challenging thanks to the precious, radioactive nature of the target metal, whose handling presents challenges far more complex than those faced with stable targets. The first daughter of ^{226}Ra , ^{219}Rn , is an inert, diffusible gas in standard ambient conditions, leading to significant radioactive

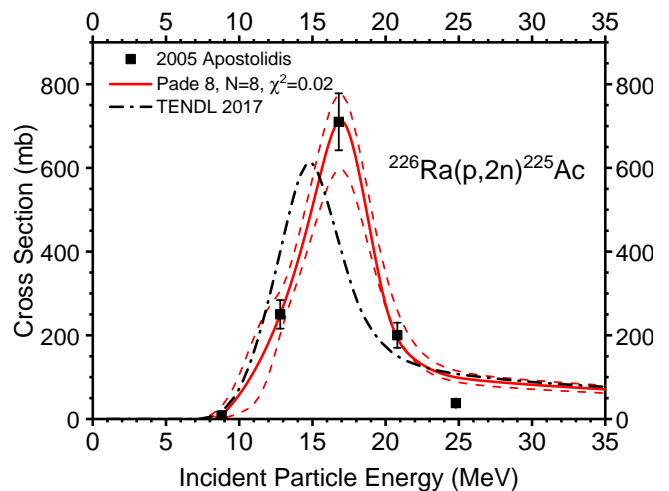


FIG. 13. Apostolidis et al. [52] data with Padé 8 Fit constrained by the predictions of the TALYS code above 30 MeV.

contamination hazards and requiring atmospheric management of alpha-emitting radionuclides in environments where the 10^2 mg targets must be chemically processed and quantitatively recovered between irradiations. The previous CRP [4] evaluated this work, so the current recommendation is primarily a revision of the fitting to update the fitting methodology. Experimental corroboration of Apostolidis *et al.*'s data becomes increasingly valuable as the demand for ^{225}Ac grows. The small number of data points available, combined with a non-physical (unreasonable low) value measured near 25 MeV, motivated evaluators' to fit the data shown in Figure 13 with the additional constraint of the theoretical predictions of the TENDL-2017 archive at energies above 30 MeV.

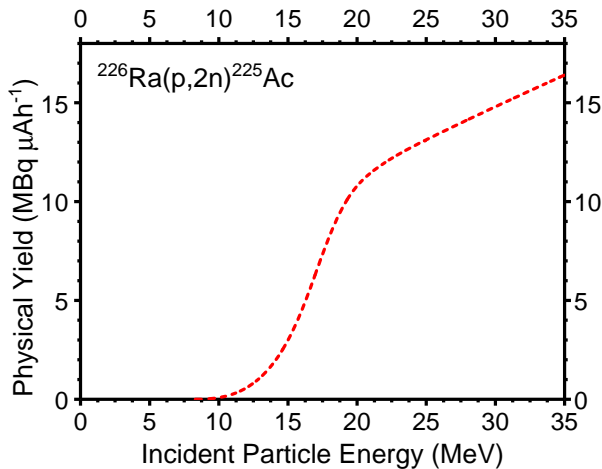
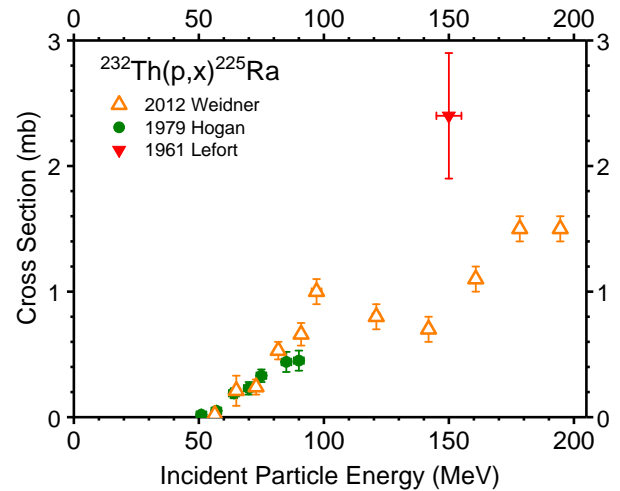


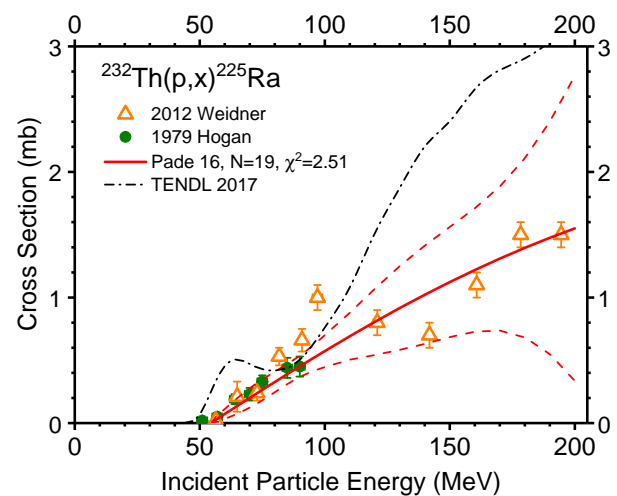
FIG. 14. (Color online) Physical yields calculated from Padé fit of data selected for the $^{226}\text{Ra}(p,2n)^{225}\text{Ac}$ reaction.

C. $^{232}\text{Th}(p,x)^{225}\text{Ra}$ (100% β^- decay) ^{225}Ac

As described above, it is also possible to produce ^{225}Ac indirectly by formation of its radioactive parent ^{225}Ra . This option is particularly interesting for production of radioisotopically pure ^{225}Ac , since direct production by high-energy proton irradiation of ^{232}Th targets leads unavoidably to the coproduction of ^{227}Ac in quantities that are concerning from a dosimetric perspective (the $^{232}\text{Th}(p,x)^{227}\text{Ac}$ reaction is discussed in detail below in the context of ^{227}Th production for ^{223}Ra). Only 6 datasets were found [41, 45, 47, 48, 53]. Of these, only three contained data below 200 MeV in the range of this evaluation; these are shown in Figure 15(a). The lack of data is likely because of the challenge of spectrometric quantification of the primary radioactive emissions of ^{225}Ra (30.0% 40 keV γ , 69.5% 316 keV β^- , and 30.5% 356 keV β^-), which are difficult to detect amid the decay emissions of its radioactive daughters. The most reliable means of quantification is by logging the more easily-observed gamma-rays of ^{221}Fr or ^{213}Bi . These data are then fit to Bateman equation models of the decay chain's equilibrium, with parameters that quantify the activities of each radionuclide in the chain. This method, however, requires



(a) All experimental data are plotted with uncertainties.



(b) Selected data compared with evaluated Padé fit and TENDL-2017 data up to 35 MeV.

FIG. 15. (Color online) Evaluated Padé fit and TENDL-2017 evaluation are compared with experimental data from Ref. [45, 48, 53] for the $^{232}\text{Th}(p,x)^{225}\text{Ra}$ reaction.

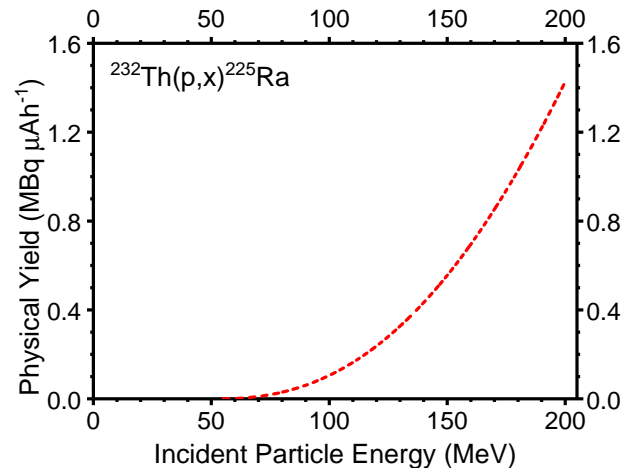


FIG. 16. (Color online) Physical yields calculated from Padé fit of data selected for the $^{232}\text{Th}(p,x)^{225}\text{Ra}$ reaction.

careful HPGe spectrometry over a period spanning weeks to achieve useful statistical certainty.

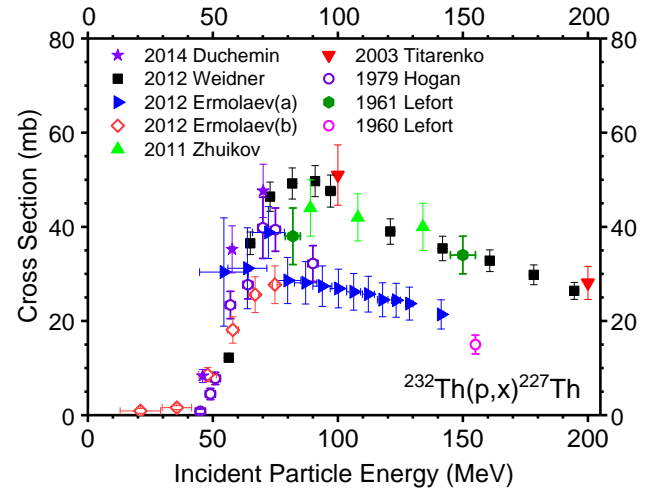
Of the datasets evaluated, 2 contained data only above 200 MeV [41, 47]. These data were used to constrain the Padé fit shown in Figure 15(b) but no recommendation is made above 200 MeV because of the overall sparseness of measured data at higher energies. One of the remaining three datasets contained only a single point [45] and was obviously discrepant from other measurements, so it was deselected (Figure 15(a)). The remaining two datasets are enough only to provide for a recommendation with high uncertainty that increases with energy up to 200 MeV, but they are self-consistent [48, 53]. The uncertainties provided in by Weidner *et al.* [48] are purely statistical in nature and underestimate the random contribution to experimental error estimates. Partly for this reason, the confidence bands associated with the Padé 16 fit of the available 19 energy points widen rapidly above 100 MeV, suggesting that more experimental measurements are urgently needed to constrain the recommended excitation function. Yields calculated from the Padé fit are shown in Figure 16.

V. PRODUCTION OF ^{227}Th

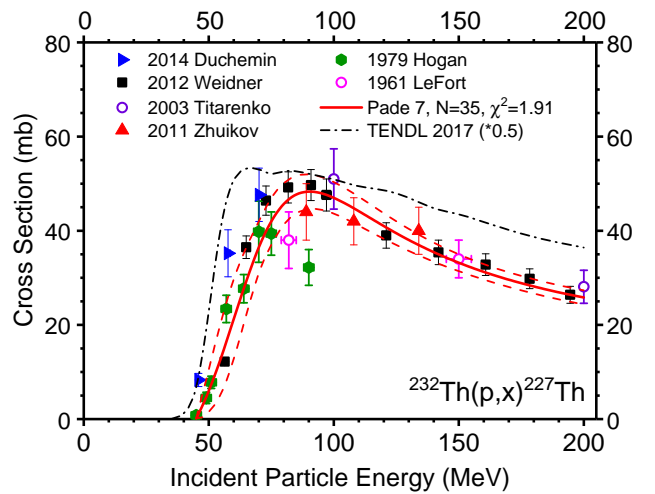
Thorium-227 ($T_{1/2} = 18.697$ d, 100% α) is being explored as a radionuclide for targeted alpha therapy in its own right and as a parent in generators of its first daughter, ^{223}Ra ($T_{1/2} = 11.43$ d, 100% α). Radium-223 is employed in its chloride form as the first U.S. Food and Drug Administration-approved alpha-emitting radiopharmaceutical. The ^{227}Th can also be obtained from a generator system thanks to the long life of its parent by β^- decay, ^{227}Ac ($T_{1/2} = 21.772$ y, 98.62% β^- , 1.38% α). Direct production by charged particle irradiations is limited by the existence of suitable stable target nuclides. The most accessible option, ^{232}Th , is of the same element as the desired product, requiring mass separation to enable use of ^{227}Th and undeveloped radiochemical isolation schemes to recover ^{223}Ra from thorium solutions containing large amounts of carrier. Indirect production of ^{227}Ac with charged particles, however, is challenging because of the need to form large amounts of ^{227}Ac in order to make useful quantities of ^{227}Th available in a timely fashion. In addition to the charged particle-induced routes examined by this CRP, neutron initiated reactions, especially the $^{226}\text{Ra}(2n,\gamma)$ family of reactions, leverage available large neutron fluxes and the relative simplicity of reactor targetry to produce useful quantities of ^{227}Ac following multiple neutron captures and β^- decays.

A. $^{232}\text{Th}(p,x)^{227}\text{Th}$

Direct production of ^{227}Th by proton irradiation of ^{232}Th requires proton energies in excess of 50 MeV. There are nine measurements of this excitation function in eight



(a) All experimental data are plotted with uncertainties.



(b) Selected data compared with evaluated Padé fit and TENDL-2017 data up to 200 MeV.

FIG. 17. (Color online) Evaluated Padé fit and TENDL-2017 evaluation are compared with experimental data from Ref. [43, 45, 47–51, 53] for the $^{232}\text{Th}(p,x)^{227}\text{Th}$ reaction. TENDL-2017 data are scaled in magnitude with the factor shown to enable comparison with measured data.

papers [43, 45, 47–51, 53], as plotted in Figure 17(a). There is clear agreement between five of the datasets which extend above 100 MeV [45, 47, 48, 50, 53], while three measurements from Refs. [43, 49] are in disagreement with all of the data. As in previous studies above, the data of Ermolaev *et al.* [49] were rejected because they used thorium targets of much larger thicknesses than are usually irradiated in stacked-foil experiments, while the single data point from Lefort *et al.* [43] was removed as an outlier due to concerns over the monitor reactions used to quantify the incident proton fluence. Remaining selected data are shown in Figure 17(b) alongside the 7 parameter Padé fit and equivalent data from TENDL-2017. The evaluated excitation function peaks between 80 and 90 MeV at 40 mb before a moderate descent to approximately 25 mb at 200 MeV. Relative uncertainties in the fit include a

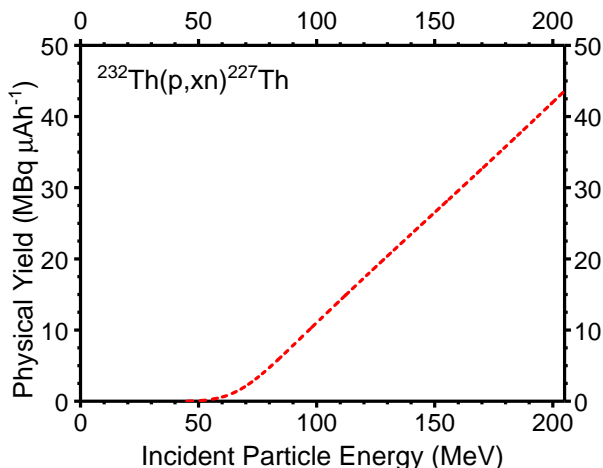
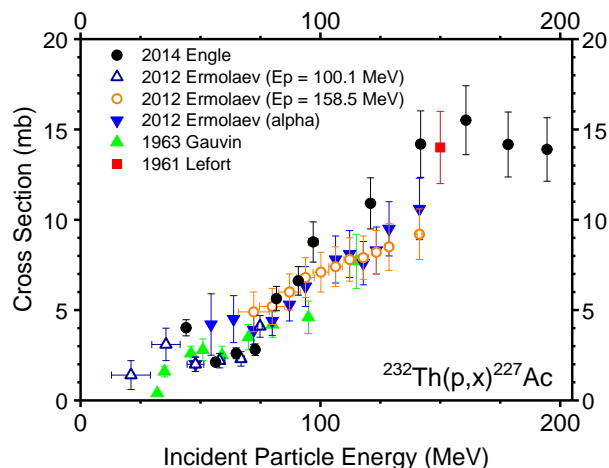


FIG. 18. (Color online) Physical yields calculated from Padé fit of data selected for the $^{232}\text{Th}(p,x)^{227}\text{Th}$ reaction.

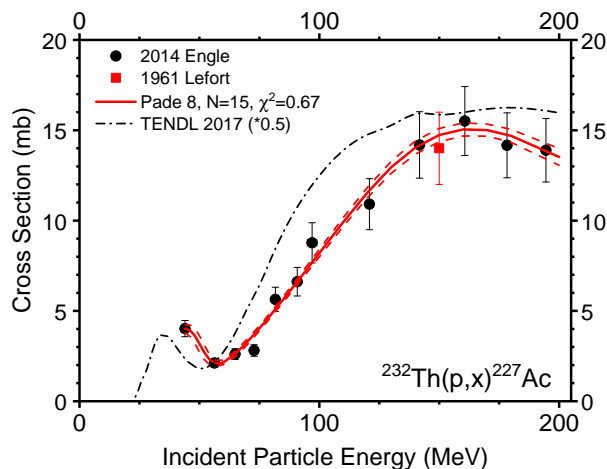
4% systematic contribution, and range from 100% of the recommended values near threshold to $7 \pm 1\%$ between 80 and 200 MeV. Physical yields increase monotonically from 80 MeV to beyond the energy range considered in these studies (see Figure 18).

B. $^{232}\text{Th}(p,x)^{227}\text{Ac}$ (98.62% β^- decay) ^{227}Th

The $^{232}\text{Th}(p,x)^{227}\text{Ac}$ reaction is described by 4 literature reports [42, 45, 49, 54], which are summarized in Figure 19(a). This reaction is important not only as an option for the production of n.c.a. ^{227}Th , but also for consideration of ^{227}Ac radioisotopic impurity that is unavoidably produced in high energy proton irradiations of ^{232}Th . The measured function displays in all cases structure corresponding to alpha exit channels below 70 MeV, but all reports disagree on the magnitude and energy location of this reaction feature. As a result, the threshold behavior of the excitation has not been accurately quantified by experiment. The data from Ermolaev et al. [49] are deselected as described multiple times previously. Experiments conducted by Gauvin [42] used values of the monitor reactions $^{27}\text{Al}(p,x)^{24}\text{Na}$ and $^{12}\text{C}(p,x)^{11}\text{C}$ which disagree by as much as 60% with modern accepted values below 60 MeV and by 10-30% between 60 and 100 MeV, so these data were also deselected. The remaining data from Refs. [45, 54] are shown in Figure 19(b) along with the data from the TENDL 2017 library and the 8 parameter Padé fit ($\chi^2=0.67$). Recommended uncertainties are below 9% across the range of energies considered, but additional experimental measurements are clearly needed to constrain the excitation function, especially near the reaction threshold where the CRP is unable to recommend numerical values. The physical yield calculated from the Padé fit, extrapolated to threshold, is shown in Figure 20.



(a) All experimental data are plotted with uncertainties.



(b) Selected data compared with evaluated Padé fit and TENDL-2017 data up to 200 MeV.

FIG. 19. (Color online) Evaluated Padé fit and TENDL-2017 evaluation are compared with experimental data from Refs. [42, 45, 49, 54] for the $^{232}\text{Th}(p,x)^{227}\text{Ac}$ reaction. TENDL-2017 data are scaled in magnitude with the factor shown to enable comparison with measured data.

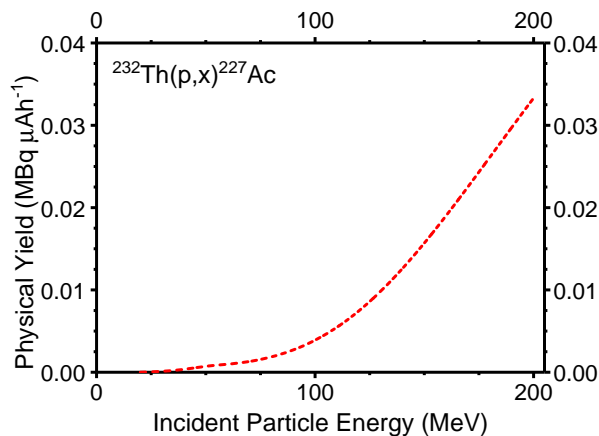


FIG. 20. (Color online) Physical yields calculated from Padé fit of data selected for the $^{232}\text{Th}(p,x)^{227}\text{Ac}$ reaction.

VI. PRODUCTION OF ^{230}U

Of the alpha-emitting radionuclides examined by this CRP, ^{230}U ($T_{1/2} = 20.8$ d, 100% α) and its short-lived daughter ^{226}Th ($T_{1/2} = 30.57$ min, 100% α) have received the least clinical attention. Unlike ^{225}Ac and ^{227}Th , there are no convenient, neutron initiated routes that lead to ^{230}U . Direct production of ^{230}U by charged particle irradiation is possible using targets of radioactive ^{231}Pa ($T_{1/2} = 32760$ y, 100% α), which is a decay product of the ^{235}U chain, and this target is examined with proton and deuteron initiated reactions below. A less efficient route is also examined, using the small β^- branch of ^{230}Pa ($T_{1/2} = 17.4$ d, 92.20% EC, 7.80% β^- , 0.0032% α), which forms ^{230}U by its decay.

A. $^{231}\text{Pa}(p,2n)^{230}\text{U}$

The difficulty of obtaining and using targets of ^{231}Pa has limited experimental measurement to a single report by Morgenstern *et al.* [55]. This publication, explores both proton and deuteron induced reactions; the latter is considered below. The 20 data points from the $^{231}\text{Pa}(p,2n)^{230}\text{U}$ reaction were fit with a 5 parameter Padé approximation without adjustment and are shown together with data from the TENDL 2017 evaluated library in Figure 21. The data cover the excitation function from threshold to energies above the peak of the $(p,2n)$ reaction, with maximum values at approximately 30 mb at 14 MeV. The uncertainty in the fit is highest near threshold, where values approach 20% of the excitation function magnitude, including a systematic contribution of 5% added throughout. At higher energies, the uncertainty does not exceed 10% with a small global minimum of approximately 8% near 20 MeV. Physical yields calculated from the Padé fit are shown in Figure 22, rising from the excitation function threshold to over $0.35 \text{ MBq}\cdot\mu\text{Ah}^{-1}$ at 25 MeV.

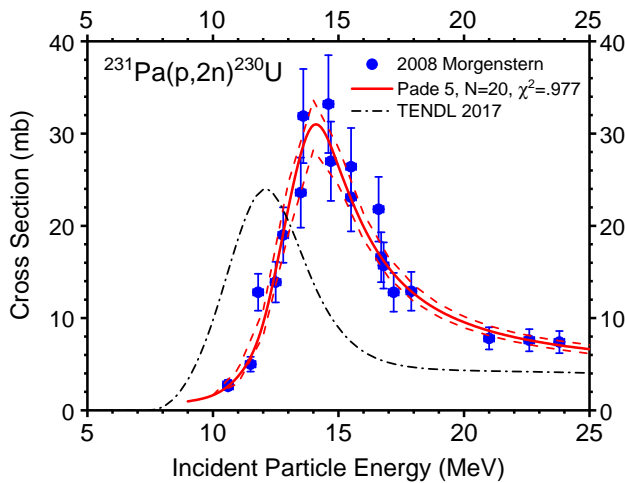


FIG. 21. Evaluated data from [55] compared with Padé fit and TENDL 2017 data.

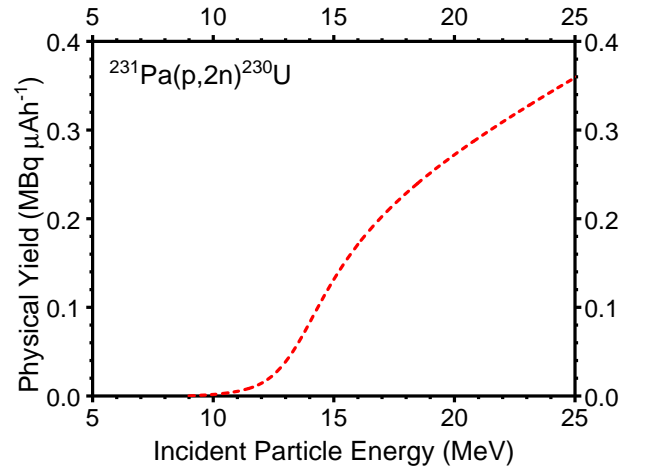


FIG. 22. (Color online) Physical yields calculated from Padé fit of data selected for the $^{231}\text{Pa}(p,2n)^{230}\text{U}$ reaction.

B. $^{231}\text{Pa}(d,3n)^{230}\text{U}$

The deuteron initiated reaction $^{231}\text{Pa}(d,3n)^{230}\text{U}$, also measured only by Morgenstern *et al.* [56] between threshold and 20 MeV, has a slightly smaller magnitude and wider peak than the $(p,2n)$ reaction described immediately above. The measured data were fit with an 8 parameter Padé approximation ($\chi^2=0.170$), which is shown in Figure 23 along with data from the TENDL-2017 evaluated library. The theoretical model significantly overestimates the magnitude of the excitation function and underestimates its peak energy by approximately 3 MeV. Uncertainty in the Padé fit is dominated by systematic contributions of 5% thanks to the measured data points' functional smoothness across the energy range explored.

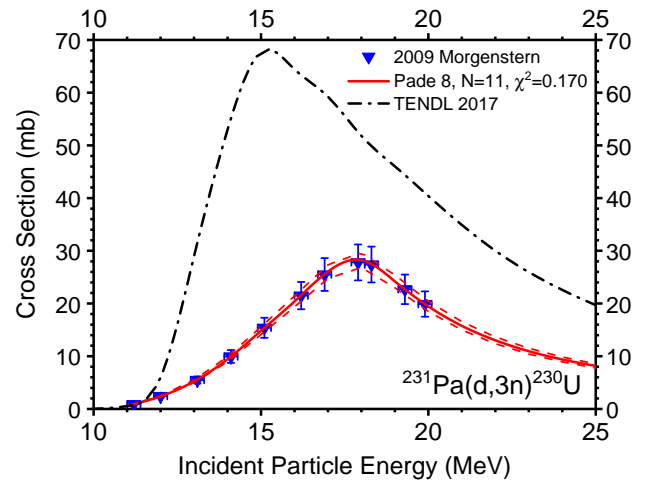


FIG. 23. Evaluated data from [56] compared with Padé fit.

Yields are calculated from the fit and shown in Figure 24, rising monotonically from threshold to a maximum of $0.25 \text{ MBq}\cdot\mu\text{Ah}^{-1}$ at 25 MeV.

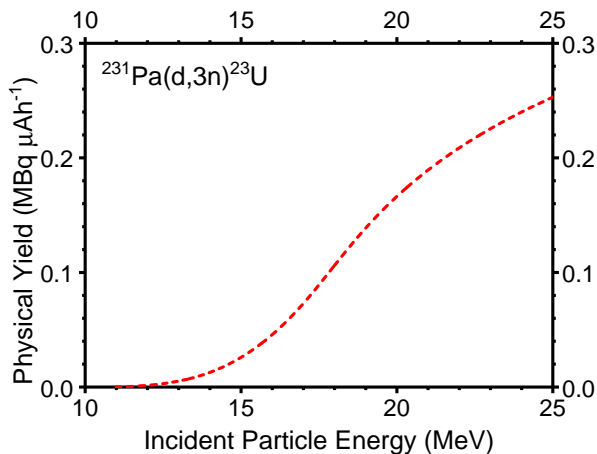
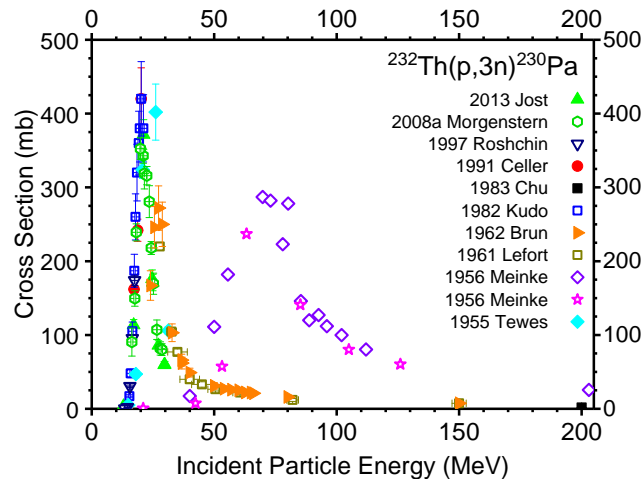


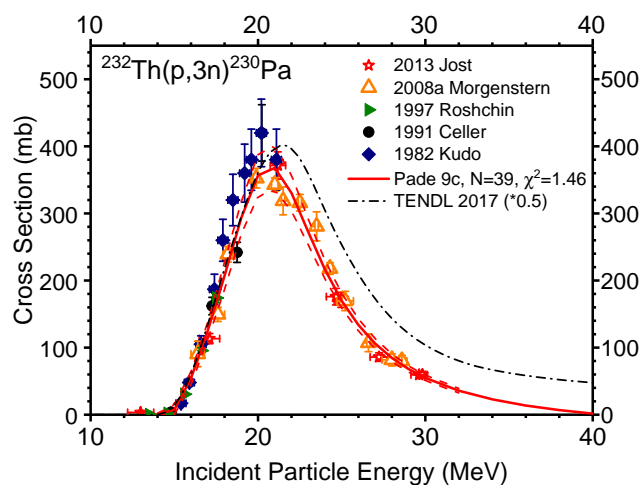
FIG. 24. (Color online) Physical yields calculated from Padé fit of data selected for the $^{231}\text{Pa}(d,3n)^{230}\text{U}$ reaction.

C. $^{232}\text{Th}(p,3n)^{230}\text{Pa}$ (7.80% β^- decay) ^{230}U

Because of the relative accessibility of ^{232}Th targets (as compared with ^{231}Pa), more data is available to describe the $^{232}\text{Th}(p,3n)^{230}\text{Pa}$ reaction than for $^{231}\text{Pa}(d,3n)^{230}\text{U}$ or $^{231}\text{Pa}(p,2n)^{230}\text{U}$. Eleven datasets dating to 1955 have quantified this excitation function up to 200 MeV [45, 57–65]. Six of these were deselected during this evaluation: Chu et al. (Ref. [64], for inaccurate monitor reactions), Brun et al. (Ref. [65], for obvious outlying data points), Lefort et al. (Ref. [45], as an obvious outlier), Meinke et al. (Ref. [58], for an approximately 50 MeV energy offset and severe outliers in data magnitude), and Tewes et al. (Ref. [57], for obvious outlying data points). These data are all shown in Figure 25(a). The remaining 39 data points from Refs. [59–63] are plotted in Figure 25(b) along with data from the TENDL-2017 evaluated library and the chosen 9 parameter Padé fit ($\chi^2=1.46$). The TENDL data overestimates the magnitude of the excitation function by a factor of two, but correctly locates its principle features in energy. Below 17 MeV, fit uncertainties range from 9–11%, but at higher energies the uncertainties decrease with increasing energy to 7% by 30 MeV. Calculated thin target physical yields from the Padé fit are more than a factor of 20 higher than yields from proton and deuteron induced reactions on ^{231}Pa targets, reaching their maximum of $8 \text{ MBq}\cdot\mu\text{Ah}^{-1}$ just above 30 MeV. This higher yield is able to account for the small branching ratio of ^{230}Pa 's β^- decay to the desired ^{230}U , and the simplicity of a target of natural abundance whose source does not involve special nuclear material makes the $^{232}\text{Th}(p,3n)^{230}\text{Pa}$ route a very attractive option compared to direct production schemes.



(a) All experimental data are plotted with uncertainties.



(b) Selected data compared with evaluated Padé fit and TENDL-2017 data up to 200 MeV.

FIG. 25. (Color online) Evaluated Padé fit and TENDL-2017 evaluation are compared with experimental data from Refs. [45, 57–65] for the $^{232}\text{Th}(p,3n)^{230}\text{Pa}$ reaction. TENDL-2017 data are scaled in magnitude with the factor shown to enable comparison with measured data.

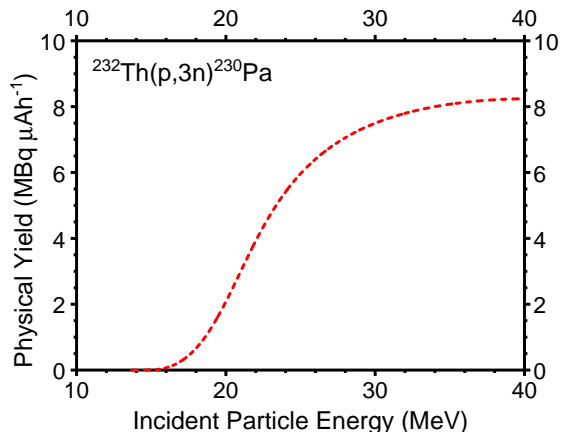


FIG. 26. (Color online) Physical yields calculated from Padé fit of data selected for the $^{232}\text{Th}(p,3n)^{230}\text{Pa}$ reaction.

VII. SUMMARY AND CONCLUSIONS

This is the final cross-section evaluation recommended by the IAEA Coordinated Research Project on Nuclear Data for Charged-particle Monitor Reactions and Medical Isotope Production. This collaborative effort galvanized nuclear cross-section research activities between 2012 and 2017 on the production of a variety of positron-, gamma-, electron-, and alpha-emitting radionuclides. The organization of such a program of work catalyzed comprehensive technical discussions of the experimental and theoretical challenges in such measurements, theoretical modeling and evaluations and incited the development of an updated set of nuclear reaction and decay data. In particular, the recommended reaction data is notable for its inclusion of uncertainties, which are expected to be broadly useful to researchers and communities seeking to standardize their own measurement programs and to strategically undertake the measurement of additional data. In this regard, the efforts of the CRP have built usefully on the previous IAEA TRS 473 published almost 8 years earlier [4].

The inclusion of data on the production of therapeutic radionuclides portends the increasing medical interest in using physically unstable nuclides as molecularly targeted vectors for the treatment of human disease. In many cases, including several discussed in this work, successful application of charged particle beams to the production of therapeutic radionuclides in clinical practice relies heavily on a balanced consideration of the nuclear data to inform yield and purity predictions which directly influence the achievable scale of clinical trials and patient dosimetry. The data and uncertainties recommended here not only serve to guide the development of infrastructure which will address global supply deficiencies of these radionuclides, but also to motivate additional studies of nuclear reactions where existing data is obviously insufficiently accurate or precise. More work is needed in many areas. Several reactions evaluated here are treated with only a single experimental measurement. The $^{226}\text{Ra}(p,2n)^{225}\text{Ac}$ in particular, as well as reactions to produce ^{227}Th , are in need of new measurements whose significance will grow

as more successful treatments of previously refractory disease are reported. Nuclear decay data evaluations and nuclear reaction characterization are both becoming increasingly important for Auger- and low energy electron-emitting radionuclides like ^{119}Sb , ^{103}Pd , and ^{135}La , and new theranostic imaging surrogates are being explored for alpha-emitting radionuclides, since the large ionic radii typical of actinide elements make it difficult for established positron-emitting nuclides to act as chemically identical congeners in low molecular weight targeting vectors which show such promise for the treatment of disease. It will also become more important in coming years to contemplate the production of therapeutic radionuclides using higher mass projectile bombardments – reactions which use beams of ionic lithium, beryllium, boron, carbon, nitrogen, etc... often have excitation functions with maxima at the hundred-millibarn scale, potentially enabling production of Gigabecquerel quantities of, e.g., ^{149}Tb for clinical applications.

Recommended therapeutic radionuclide production reaction data and their uncertainties are available on the Web page of the IAEA NDS at www-nds.iaea.org/radionuclides/ and also at the IAEA medical portal www-nds.iaea.org/medportal/.

ACKNOWLEDGEMENTS

Our sincere thanks to all colleagues who have contributed to and worked on this project during the last five years. The preparation of this paper would not have been possible without the support and effort of a large number of institutions and individuals. The IAEA is grateful to all participant laboratories for their assistance in the work and for support of the CRP meetings and activities. The work described in this paper would not have been possible without IAEA Member State contributions. Work at Argonne National Laboratory and Los Alamos National Laboratory was supported by the U.S. Department of Energy, Office of Science, Office of Nuclear Physics. We further acknowledge the valuable contributions made by I. Spahn from FZK Julich, Germany, during various project meetings.

-
- [1] S.M. Qaim, “Therapeutic Radionuclides and Nuclear Data”, *RADIOCHIM. ACTA* **89**, 297–302 (2011).
- [2] S.M. Qaim, “Nuclear Data for Medical Radionuclides”, *J. RADIOANAL. NUCL. CHEM.* **305**, 233–245 (2015).
- [3] S.M. Qaim, “Nuclear Data for Production and Medical Application of Radionuclides: Present Status and Future Needs”, *NUCL. MED. BIOL.* **44**, 31–49 (2017).
- [4] E. Běták, A.D. Caldeira, R. Capote, B.V. Carlson, H.D. Choi, F.B. Guimarães, A.G. Ignatyuk, S.K. Kim, B. Király, S.F. Kovalev, E. Menapace, A.L. Nichols, M. Nortier, P. Pompeia, S.M. Qaim, B. Scholten, Yu.N. Shubin, J.-Ch. Sublet and F. Tárkányi, “Nuclear Data for the Production of Therapeutic Radionuclides”, **IAEA Technical Reports Series No. 473**, Eds: S.M. Qaim, F. Tárkányi and R. Capote, International Atomic Energy Agency, Vienna, Austria, 2011, ISBN 978-92-0-115010-3. Available online at www-nds.iaea.org/publications/tecdocs/technical-reports-series-473.pdf.
- [5] R. Capote and F.M. Nortier, Consultants’ Meeting on “Improvements in charged-particle monitor reactions and nuclear data for medical isotope production”, 21–24 June 2011, IAEA report **INDC(NDS)-0591**, September 2011, IAEA, Vienna, Austria. Available online at www-nds.iaea.org/publications/indc/indc-nds-0591.pdf.

- [6] A.L. Nichols, S.M. Qaim and R. Capote, Technical Meeting on “Intermediate-term Nuclear Data Needs for Medical Applications: Cross Sections and Decay Data”, 22-26 August 2011, IAEA report **INDC(NDS)-0596**, September 2011, IAEA, Vienna, Austria. Available online at www.nds.iaea.org/publications/indc/indc-nds-0596.pdf.
- [7] A.L. Nichols and R. Capote, Summary Report of First Research Coordination Meeting on Nuclear Data for Charged-particle Monitor Reactions and Medical Isotope Production, 3-7 December 2012, IAEA report **INDC(NDS)-0630**, February 2013, IAEA, Vienna, Austria. Available online at www.nds.iaea.org/publications/indc/indc-nds-0630.pdf.
- [8] A.L. Nichols, F.M. Nortier and R. Capote, Summary Report of Second Research Coordination Meeting on “Nuclear Data for Charged-particle Monitor Reactions and Medical Isotope Production”, 8-12 December 2014, IAEA report **INDC(NDS)-0675**, April 2015, IAEA, Vienna, Austria. Available online at www.nds.iaea.org/publications/indc/indc-nds-0675.pdf.
- [9] A.L. Nichols, F.M. Nortier and R. Capote, Summary Report of Third Research Coordination Meeting on “Nuclear Data for Charged-particle Monitor Reactions and Medical Isotope Production”, 30 May-3 June 2016, IAEA report **INDC(NDS)-0717**, January 2017, IAEA, Vienna, Austria. Available online at www.nds.iaea.org/publications/indc/indc-nds-0717.pdf.
- [10] A. Hermanne, A. V. Ignatyuk, R. Capote, B.V. Carlson, J.W.Engle, M.A. Kellett, T. Kibédi, G. Kim, F. G. Konddev, M. Hussain, O. Lebeda, A. Luca, Y. Nagai, H. Naik, A. L. Nichols, F.M. Nortier, S.V. Suryanarayana, S. Takács, F.T. Tarkányi, and M. Verpelli, “Reference Cross Sections for Charged-particle Monitor Reactions”, **NUCL. DATA SHEETS****148**, 328-382 (2018).
- [11] H.E. Padé, “Sur la Représentation Approchée d’ une Fonction par des Fractions Rationnelles”, Supplement to **ANN. SCI. L’ÉCOLE NORM. SUP.**, Series 3, Vol. **9**, 3-93 (1892).
- [12] P.R. Graves-Morris (Ed.), “Padé Approximants and their Applications”, Academic Press, New York (1973).
- [13] G.A. Baker Jr., “Essentials of Padé Approximants”, Academic Press, New York (1975).
- [14] V.N. Vinogradov, E.V. Gai and N.S. Rabotnov, “Analytical Approximation of Data in Nuclear and Neutron Physics”, Energoatomizdat, Moscow (1987); in Russian.
- [15] E.V. Gai, “Some Algorithms for the Nuclear Data Evaluation and Construction of the Uncertainty Covariance Matrices”, *Vopr. Atomnoy Nauki i Tekhniki, ser. Nuclear Constants*, Issues **1-2**, 56-65 (2007); in Russian.
- [16] **NuDat**, Brookhaven National Laboratory, USA. Decay data retrieval code available online at www.nndc.bnl.gov/nudat2/.
- [17] Evaluated Nuclear Structure Data File (ENSDF). Available online at www.nndc.bnl.gov/ensdf/. Developed and maintained by the International Network Of Nuclear Structure and Decay Data Evaluators (NSDD) (see www.nds.iaea.org/nsdd/).
- [18] U.K. Henschke, and D.C. Lawrence, “Cesium-131 seeds for permanent implants”, **RADIOL.** **85**, 1117 (1965).
- [19] T.S. Kehwar, “Use of Cesium-131 radioactive seeds in prostate permanent implants”, **J. MED. PHYS.** **34**, 191 (2009).
- [20] S. Pommé, M. Marouli, G. Suliman, H. Dikmen, R. Van Ammel, V. Jobbágy, A. Dirican, H. Stroh, J. Paepen, F. Bruchertseifer, C. Apostolidis, A. Morgenstern, “Measurement of the ^{225}Ac half-life.” **APP. RAD. ISOTOP.**, **70**(11), 2608 (2012)
- [21] F. Tarkanyi, A. Hermanne, S. Takacs, R.A. Rebeles, P. Van den Winkel, B. Kiraly, F. Ditroi, A.V. Ignatyuk, “Cross section measurements of the $^{131}\text{Xe}(p,n)$ reaction for production of the therapeutic radionuclide ^{131}Cs .” **APP. RAD. ISOTOP.**, **67**, 1751 (2009).
- [22] M.C. Lagunas-Solar, F.E. Little, and H.A. Moore, Jr., “Cyclotron Production of ^{128}Cs (3.62 min). A New Positron-Emitting Radionuclide for Medical Applications”, **APPL. RADIAT. ISOT.** **33**, 619 (1982); EXFOR C0968.
- [23] C. Deptula, Kim Sen Han, O. Knotek, S. Mikolajewski, L.M. Popinenkova, E. Rurarz, and N.G. Zaitseva, “Production of $^{128,131}\text{Ba}$, ^{132}Cs in proton induced reactions on a Cs target and of $^{127,129}\text{Cs}$ in $^3,^4\text{He}$ induced reactions on I target.”, **NUKLEONICA** **35**, 63 (1990); EXFOR A0572.
- [24] R.W. Fink and E.O. Wiig, “Reactions of Cesium with Protons at 60, 80, 100, 150, and 240 MeV”, **PHYS. REV.** **96**, 185 (1954); EXFOR C2000.
- [25] F. Tarkanyi, A. Hermanne, S. Takacs, F. Ditroi, B. Kiraly, H. Yamazaki, M. Baba, A. Mohammadi, and A.V. Ignatyuk, “New measurements and evaluation of excitation functions for (p,xn) , (p,pxn) and $(p,2pxn)$ reactions on ^{133}Cs up to 70 MeV proton energy”, **APPL. RADIAT. ISOT.** **68**, 47 (2010); EXFOR D4226.
- [26] R. S. Tilbury and L. Yaffe, “ ^{131m}Ba - A new isomer”, **PHYS. REV.** **129**, 1709 (1963); EXFOR D4224.
- [27] K. Sakamoto, M. Dohniwa, and K. Okada, “Excitation Function for (p,xn) and (p,pxn) Reactions on Natural $^{79+81}\text{Br}$, $^{85+87}\text{Rb}$, ^{127}I and ^{133}Cs up to $E_p = 52$ MeV”, **APPL. RADIAT. ISOT.** **36**, 481 (1985); EXFOR E1867.
- [28] R.D. Neirinckx, B.L. Holman, M.A. Davis, R.E. Zimmerman, “Tantalum-178 radiopharmaceuticals for lung and liver imaging.” **JOURN. NUCL. MED.**, **20**, 1176 (1978a).
- [29] R.D. Neirinckx, A.G. Jones, M.A. Davis, G.I. Harris, B.L. Holman, “Tantalum-178 - A short lived nuclide for nuclear medicine: Development of a potential generator system.” **JOURN. NUCL. MED.**, **19**, 514 (1978b).
- [30] B.L. Holman, G.I. Harris, R.D. Neirinckx, A.G. Jones, J. Idoine, “Tantalum-178 - A short lived nuclide: Production of the parent W-178.” **JOURN. NUCL. MED.**, **19**, 510 (1978).
- [31] C.J. Hartley, J.L. Lacy, D. Dai, N. Nayak, G.E. Taffet, M.L. Entman, L.H. Michael, “Functional cardiac imaging in mice using Ta-178.” **NATURE MEDICINE**, **5**, 237 (1999).
- [32] J. Bisplinghoff, J. Ernst, T. Mayer-Kuckuk, P. Jahn, C. Mayer-Boericke, “Excitation Functions of D-Induced Reactions on ^{181}Ta from 10 to 80 MeV and Equilibrium Statistical Analysis of (p,xn) Reactions on Tantalum and Gold.” **NUCL. PHYS. A**, **2281**, 180 (1974).
- [33] F. Tarkanyi, S. Takacs, F. Ditroi, A. Hermanne, A.V. Ignatyuk, M.S. Uddin, “Activation cross sections of a-particle induced nuclear reactions on hafnium and deuteron-induced nuclear reaction on tantalum: Production of $^{178}\text{W}/^{178m}\text{Ta}$ generator.” **APP. RAD. ISOTOP.**, **91**, 114 (2004).
- [34] G. Kim, M. Shahid, K. Kim, M. Zaman, M. Tatari, S. Yang, H. Naik, “Measurement of excitation functions for the $^{nat}\text{Ta}(p,x)$ reactions”, submitted to **NUCL. INSTR. METH. B**, **91** (2016).

- [35] N.G. Zaytseva, E. Rurarz, V.A. Khalkin, V.I. Stegailov, L.M. Popinenkova, "Excitation Function For W-178 Production in the Ta-181(p,4n)W-178 Reaction Over Proton Energy Range 28.8-71.8 MeV." *RADIOCHIM. ACTA*, **64**, 1 (1994).
- [36] C. Birattari, E. Gadioli, A.M. Grassi Strini, G. Strini, G. Tagliaferri, L. Zett, "(p,xn) Reactions Induced in Tm-169, Ta-181 and Bi-209 with 20 to 45 MeV Protons." *NUCL. PHYS. A*, **166**, 605 (1971).
- [37] M.S. Uddin, M. Hagiwara, N. Kawata, T. Itoga, N. Hirabayashi, M. Baba, F. Tarkanyi, F. Ditroi, J. Csikai, "Measurement of excitation functions of the proton-induced activation reactions on tantalum in the energy range 28-70 MeV." *JOURNAL. NUCL. SCI. TECH.*, **4**, 160 (2004).
- [38] R. Michel, M. Gloris, J. Protoschill, U. Herpers, J. Kuhnenn, F. Sudbrock, P. Malmberg, P. Kubik, "Cross sections for the production of radionuclides by proton-induced reactions on W, Ta, Pb and Bi from thresholds up to 2.6 GeV." *JOURNAL. NUCL. SCI. TECH.*, **2**, 242 (2002).
- [39] Yu.E. Titarenko, V.F. Batyaev, A.Yu. Titarenko, M.A. Butko, K.V. Pavlov, S.N. Florya, R.S. Tikhonov, V.M. Zhivun, A.V. Ignatyuk, S.G. Mashnik, S. Leray, A. Boudard, J. Cugnon, D. Mancusi, Y. Yariv, K. Nishihara, N. Matsuda, H. Kumawat, G. Mank, W. Gudowski, "Measurement and simulation of the cross sections for nuclide production in W-nat and Ta-181 targets irradiated with 0.04- to 2.6-GeV protons." *YADERNAYA FISIKA*, **74**, 574 (2001).
- [40] J.W. Engle, "The Production of Ac-225", *CURR. RADIOPHARM.* In Press (2018), doi: 10.21741874471011666180418141357.
- [41] M. Lindner, R.N. Osborne, "Nonfission inelastic events in uranium and thorium induced by high-energy protons." *PHYS. REV.*, **103**(2), 387 (1956).
- [42] H. Gauvin, "Reactions (p,2p α n) sur le thorium-232 de 30 a 120 MeV." *JOURNAL. PHYSIQUE*, **24**, 386 (1963).
- [43] M. Lefort, G. Simonoff, X. Tarrago, "Competition fission-spallation dans les cibles de thorium bombardees par proton de 155 MeV." *J. PHYS. RADIUM*, **21**, 388 (1960).
- [44] B.D. Pate, A.M. Poskanzer, "Spallation of uranium and thorium nuclei with BeV-energy protons." *PHYS. REV.*, **123**(2), 647 (1961).
- [45] M. Lefort, G.N. Simonoff, X. Tarrago, "A spallation nuclear reaction on thorium at 150 and 82 MeV proton energies." *NUCL. PHYS.*, **254**, 216 (1961).
- [46] J.R. Griswold, D.G. Medvedev, J.W. Engled, R. Copping, J.M. Fitzsimmons, V. Radchenko, J.C. Cooley, M.E. Fassbender, D.L. Denton, K.E. Murphy, A.C. Owens, E.R. Birnbaum, K.D. John, F.M. Nortier, D.W. Stracener, L.H. Heilbronn, L.F. Mausner, S. Mirzadeh, "Large scale accelerator production of ^{225}Ac : Effective cross sections for 78192 MeV protons incident on ^{232}Th targets", *APP. RAD. ISOTOP.*, **118**, 366-374 (2016).
- [47] E. Titarenko, V.F. Batyaev, E.I. Karpikhin, R.D. Mulambetov, A.B. Koldobsky, V.M. Zhivun, S.V. Mulambetova, K.A. Lipatov, U.A. Nekrasov, A.V. Belkin, N.N. Alexeev, V.A. Schegolev, Y.M. Goryachev, V.E. Luk'yashin, E.N. Firsov, "Experimental and theoretical study of the yields of residual product nuclei produced in thin targets irradiated by 100-2600 MeV protons." *INDC (CCP)-434*, Technical Report of the International Science and Technology Center Project No. 839B-99, IAEA, Vienna, 2003.
- [48] J.W. Weidner, S.G. Mashnik, K.D. John, B. Ballard, E.R. Birnbaum, L.J. Bittker, A. Couture, M.E. Fassbender, G.S. Goff, R. Gritz, F.M. Hemez, W. Runde, J.L. Ullmann, L.E. Wolfsberg, F.M. Nortier, "Proton-induced cross sections relevant to production of ^{225}Ac and ^{223}Ra in natural thorium targets below 200 MeV," *APP. RAD. ISOTOP.*, **70**, 2602 (2012).
- [49] S.V. Ermolaev, B.L. Zhuikov, V.M. Kokhanyuk, V.L. Matushko, S.N. Kalmykov, R.A. Aliev, I.G. Tananaev, B.F. Myasoedov, "Production of actinium, thorium and radium isotopes from natural thorium irradiated with protons up to 141 MeV." *RADIOCHIMICA ACTA*, **100**, 223 (2012).
- [50] B.L. Zhuikov, S.N. Lalmykov, S.V. Ermolaev, R.A. Aliev, V.M. Kokhanyuk, V.L. Matushko, I.G. Tananaev, B.F. Myasoedov, "Production of ^{225}Ac and ^{223}Ra by irradiation of Th with accelerated protons." *RADIOCHEMISTRY*, **53**(1), 73-80 (2011).
- [51] C. Duchemin, A. Guertin, F. Haddad, N. Michel, V. Metivier, "Production of medical isotopes from a thorium target irradiated by light charged particles up to 70 MeV." *PHYS. MED. BIOL.* **60**, 931, 2015.
- [52] C. Apostolidis, R. Molinet, J. McGinley, K. Abbas, J. Mollenbeck, A. Morgenstern, "Cyclotron production of Ac-225 for targeted alpha therapy." *APP. RAD. ISOTOP.*, **62**, 383 (2005).
- [53] J.J. Hogan, E. Gadioli, E. Gadioli-Erba, C. Chung, "Fissionability of Nuclides in the Thorium Region at Excitation Energies to 100 MeV." *PHYS. REV. C*, **20**, 1831 (1979).
- [54] J.W. Engle, J.W. Weidner, B.D. Ballard, M.E. Fassbender, L.A. Hudston, K.R. Jackman, D.E. Dry, L.E. Wolfsberg, L.J. Bittker, J.L. Ullmann, M.S. Gulley, C. Pillai, G. Goff, E.R. Birnbaum, K.D. John, S.G. Mashnik, F.M. Nortier, "Ac, La, and Ce radioimpurities in ^{225}Ac produced in 40-200 MeV proton irradiations of thorium." *RADIOCHIM. ACTA*, **201**(7), 569-581(2014).
- [55] A. Morgenstern, O. Lebeda, J.A. Tursa, F. Bruchertseifer, R. Capote, J. McGinley, G. Rasmussen, M. Sin, B. Zielinska, Ch. Apostolidis, "Production of $^{230}\text{U}/^{226}\text{Th}$ for targeted alpha therapy via proton irradiation of ^{231}Pa ." *ANAL. CHEM.*, **80**, 22 (2008).
- [56] A. Morgenstern, O. Lebeda, J.A. Tursa, R. Capote, M. Sin, F. Bruchertseifer, B. Zielinska, C. Apostolidis, "Cross sections of the reaction $^{231}\text{Pa}(d,3n)^{230}\text{U}$ for production of $^{230}\text{U}/^{226}\text{Th}$ for targeted alpha therapy." *PHYS. REV. C*, **80**(5), 054612 (2009).
- [57] H.A. Tewes, "Excitation Functions for Some Proton-Induced Reactions of Thorium." *PHYS. REV.*, **98**, 25 (1955).
- [58] W.W. Meinke, G.C. Wick, G.T. Seaborg, "High-energy excitation functions in the heavy region." *J. INORG. NUCL. CHEM.*, **3**, 69 (1956).
- [59] A. Celler, M. Luontama, J. Kantele, J. Zylicz, "Cross Sections of $^{232}\text{Th}(p,xn+yp)$ Reactions at $E(p) = 6.8$ to 20.2 MeV." *PHYS. SCRIPTA*, **24**, 930 (1981).
- [60] H. Kudo, H. Muramatsu, H. Nakahara, K. Miyano, I. Kohno, "Fission Fragment Yields in the Fission of ^{232}Th by Protons of Energies 8 to 22 MeV." *PHYS. REV. C*, **25**, 3011 (1982).
- [61] C.U. Jost, J.R. Griswold, S.H. Bruffey, S. Mirzadeh, D.W. Stracener, C.L. Williams, "Measurement of Cross Sections for the $^{232}\text{Th}(p,4n)^{229}\text{Pa}$ Reaction At Low Proton Energies." *CONF. PROC. AM. INST. PHYS.*, **1525**, 520 (2013).

- [62] A. Roshchin, S. Yavshits, V. Jakovlev, E. Karttunen, J. Aaltonen, S. Heselius, "Cross sections of nonfission reactions induced in Th-232 by low-energy protons." *PHYS. ATOMIC NUCLEI*, **60**, 1941 (1997).
- [63] A. Morgenstern, C. Apostolidis, F. Bruchertseifer, R. Capote, T. Gouder, F. Simonelli, M. Sin, K. Abbas, "Cross-sections of the reaction $^{232}\text{Th}(p,3n)^{230}\text{Pa}$ for production of ^{230}U for targeted alpha therapy." *APP. RAD. ISO-
TOP.*, **66**, 1275 (2008).
- [64] Y. Y. Chu, M. L. Zhou, "Comparison of the (p, xn) Cross Sections from ^{238}U , ^{235}U and ^{232}Th Targets Irradiated with 200 MeV Protons", *IEEE TRANS. NUCL. SC.*, **30**, 1153–1155 (1983).
- [65] C. Brun, G.N. Simonoff, "Compétition fission-évaporation. Etude des fonctions d'excitation dans différents noyaux de protactinium", *PHYS. RAD.*, **23**, 12–16 (1962).